View Article Online
View Journal

Environmental Science Nano

Accepted Manuscript

This article can be cited before page numbers have been issued, to do this please use: V. Alcolea-Rodriguez, R. Portela, V. Calvino-Casilda and M. Bañares, *Environ. Sci.: Nano*, 2024, DOI: 10.1039/D3EN00810J.

ROYAL SOCIETY OF CHEMISTRY

rsc.li/es-nano

View Article Online
DOI: 10.1039/D3EN00810J

Data availability statements

All data supporting the findings of this study are presented in the main article and in the Supplementary Information.

Victor Alcolea-Rodriguez
Instituto de Catálisis y Petroleoquímica,
CSIC, C/ Marie Curie, 2
28049 Madrid, Spain

View Article Online
DOI: 10.1039/D3EN00810J
Environmental Science: Nano

Environmental Significance Statement

Nanomaterials hazard is associated with their surface reactivity. We report an *in chemico* approach to probe the number, nature and reactivity of surface sites. This approach tells how many sites we have at the surface of nanomaterials; relevant for a dose metric based on actual sites rather than on surface or mass. This would allow better insight on dose-response investigations. This NAM provides insights into whether sites are oxidative, acidic, basic, or a combination thereof, and additionally aids in ranking NMs by reactivity, which is crucial for understanding their mechanisms of toxicity. In a broader view, it can characterize nanomaterials and how their reactivity evolves as they change making multicomponent nanomaterials and as they age during operation and in the environment.

Spectroscopy and Industrial Catalysis group
CSIC-Instituto de Catálisis y Petroleoquímica
victor.alcolea@csic.es

Marie Curie nº2
E-28049-MADRID,
SPAIN

View Article Online
DOI: 10.1039/D3EN00810J

In chemico methodology for engineered nanomaterials categorization according to number, nature and oxidative potential of reactive surface sites

V. Alcolea-Rodriguez[a*], R. Portela[a], V. Calvino-Casilda[b], M.A. Bañares[a*]

[a] Instituto de Catálisis y Petroleoquímica, ICP-CSIC, Marie Curie 2, 28049-Madrid, Spain

[b] Departamento de Ingeniería Eléctrica, Electrónica, Control, Telemática y Química Aplicada a la Ingeniería, E.T.S. de Ingenieros Industriales, UNED, Juan del Rosal 12, 28040-Madrid, Spain

***Corresponding authors**: miguel.banares@csic.es victor.alcolea@csic.es

Keywords

Surface descriptor, chemisorption, oxidative potential, active sites, dose metrics, probe molecule, probe reaction, new approach methodologies

View Article Online
DOI: 10.1039/D3EN00810J

Abstract

Methanol probe chemisorption quantifies the number of reactive sites at the surface of engineered nanomaterials, enabling normalization per reactive site in reactivity and toxicity tests, rather than per mass or physical surface area. Subsequent *temperature-programmed surface reaction* (TPSR) of chemisorbed methanol identifies the reactive nature of surface sites (acidic, basic, redox or combination thereof) and their reactivity. Complementary to methanol assay, dithiothreitol (DTT) probe oxidation reaction is used to evaluate oxidation capacity. These acellular approaches to quantify the number, nature, and reactivity of surface sites constitute a New Approach Methodology (NAM) for site-specific classification of nanomaterials. As a proof of concept, CuO, CeO_2, ZnO, Fe_3O_4, $CuFe_2O_4$, Co_3O_4 and two TiO_2 nanomaterials were probed, and a harmonized reactive descriptor was obtained: DTT oxidation rate per reactive site, or *Oxidative Turnover Frequency* (OxTOF). CuO and $CuFe_2O_4$ nanoparticles exhibit the largest reactive sites surface density and are the most oxidative in the series, as estimated by DTT probe reaction, followed by CeO_2 NM-211 and, then, by titania nanomaterials (DT-51 and NM-101) and Fe_3O_4. DTT depletion in ZnO NM-110 was associated with dissolved zinc ions rather than the ZnO particles themselves, but the basic character of the ZnO NM-110 particles surface was evidenced by methanol TPSR. These acellular assays allow ranking the 8 nanomaterials into three categories with statistically different oxidative potential: CuO, $CuFe_2O_4$ and Co_3O_4 are the most reactive, ceria exhibits a moderate reactivity, and iron oxide and the titanias possess a low oxidative potential.

View Article Online
DOI: 10.1039/D3EN00810J

1 INTRODUCTION

The surface of engineered nanomaterials (ENMs). Metal oxides possess a lattice which unit cell repeats *ad infinitum.* However, materials are finite, and interact with the surrounding environment through their surface, the end of the lattice periodic structure, which is characterized by descriptors such as specific surface area (BET area), pore size, or zeta-potential (ζ).[1] Surface chemistry defines materials' reactivity (type and strength), in metal oxides often associated with surface oxygen species, such as bridging oxygen, oxide, superoxide, peroxide, or hydroxyl sites (**Error! Reference source not found.**), which properties are determined by underlying cations, defects, and the bulk structure. Charge unbalances such as surface vacancies, defects and others, are stabilized to keep the material neutrality, typically by surface interactions with, e.g., environmental water, generating surface hydroxyl groups. The compensation mechanisms for defects may vary depending on the nature of the material; like the formation of *farb* centers, covalent bonding or transitions between valence and conduction bands in ionic, covalent on transition element oxides, respectively[2]. Surface relevance is maximized in non-soluble nanomaterials (NMs, with one dimension in the 1-100 nm range)[3], in which a high surface-to-volume ratio confers them with distinctive properties. For example, in the field of ecotoxicology, 40 mg/L of nano-sized CuO particles completely inhibit the growth of *S. cerevisiae,* while 4000 mg/L of CuO bulk material are needed[4] ; the number of exposed sites is probably not dramatically different between these two very different amounts of CuO materials.

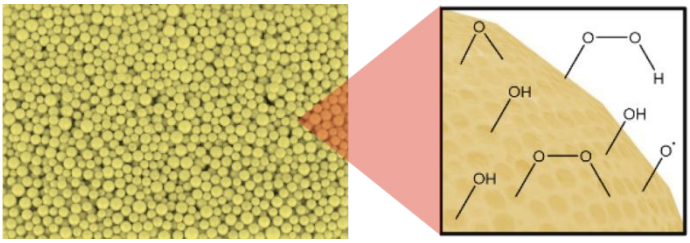

Figure 1. *Reactive sites on ENMs surface*

Rise of engineered nanomaterials and concern about their toxicity. Engineered nanomaterials applications have grown significantly, influencing societal challenges and the economy, especially in Asia-Pacific, America, and Europe.[5,6,7,] Transition metal oxide ENMs, including TiO_2, CuO, ZnO, and others, have versatile uses like pigments and catalysts.[8,9] This has prompted numerous characterization, exposure and hazard studies[10–12] to understand and prevent possible adverse effects or pathologies*, e.g.* derived from reactive

View Article Online
DOI: 10.1039/D3EN00810J

oxygen species (ROS) release,[13,14] and to adopt a knowledge-based safe-by-design (SbD) approach[15,16], essential to ensure safe ENM applications as well as faster, economic and more effective production routes.[17,18] Integrated information related to toxicity (*in vitro* and *in vivo* testing) and physicochemical properties underpins hazard prediction[16, 19, 20, 21 22 23], with machine learning serving as the primary tool.[24] Grouping ENMs based on similarities can optimize resource management, aligning with OCDE guidelines for risk assessment and promoting non-animal testing methodologies.[25,26] New approach methodologies (NAMs) may provide the basis for this objective.[27,28,29] The overarching aim is to contribute to the understanding of Adverse Outcome Pathways (AOPs) and, particularly, what reactive properties are associated with the triggering of adverse effects by nanomaterials.[30]

New approach methodology based on surface sites reactivity. Nanomaterial surface reactivity plays a vital role in oxidative-stress-induced adverse effects.[31,32,33,34] As reactivity is an extrinsic property considered a key parameter to describe the interaction of ENMs with their surroundings, [16, 19] the development of abiotic *in chemico* assays to evaluate surface reactivity and link it with key events in reactive-based nanotoxicity would help to fundamentally understand the modes of action[35,36,37] and better group ENMs while minimizing *in vivo* testing.[38] Surface reactivity characterization complements other physicochemical information relevant to the nanotoxicity field[19] to investigate toxic ion release, lung fibrosis, inflammasome activation, interference with embryonic hatching or membrane lysis, among others. In the context of reactive-based toxicity assessment of engineered nanomaterials, it is widely acknowledged that materials with identical chemical compositions can lead to significantly varied biological oxidative damage.[34] Thus, characterizing the amount, nature and reactivity of surface sites is essential for identifying an additional parameter impacting nanomaterial's effects. The interaction with biological systems depends on the surface properties of the nanomaterials, the presence of any kind of active site may have effects on their interaction with molecules. We hypothesize that mapping all reactive sites (redox, acidic and basic) may provide a better reactive description of nanomaterials than just oxidative sites, and enable a more reliable grouping of nanomaterials based on their surface reactivity. Formally equivalent problems have formally equivalent solutions: as key events in reactive-based toxicity and catalytic reactions occur at the surface, more specifically, at the reactive sites, we propose the use of catalytic methods based on adsorption and reaction of probe molecules to quantify the surface

View Article Online
DOI: 10.1039/D3EN00810J

reactive sites of ENMs and to characterize their reactive nature, thus delivering descriptors relevant for ENMs classification.[39,40]

The reactive characterization may also provide new dose metrics. In *in vitro* tests with different cell lines, quantitative dose-dependent cellular/biological effects are typically normalized by mass or physical BET area. These dose metrics may sometimes not be useful to compare exposure because mass or exposed physical area do not necessarily correlate with the number of reactive sites, which trigger chemical processes, *e.g.*, ROS formation (generation of ROS by particles is one of the possible molecular initiating events that lead to adverse outcomes, as confirmed e.g. for PM, CuO, or photo-activated TiO_2). We do not tackle photocatalytic phenomena that are unlikely to happen inside the body. Research in heterogeneous catalysis has traditionally faced the same challenge when comparing the activity of catalytic materials and has reached a consensus that the most relevant metric is the turnover frequency (TOF). TOF is the number of times that the overall catalytic reaction takes place (*i.e.*, molecules that react) per reactive site and unit time.[41,39,42,43,44] Our research posits that probe molecules will allow quantification of reactive surface sites, their nature and reactivity; TOF calculation can thus be made based on relevant probe reactions (*e.g.*, DTT), offering new metrics for reactivity and toxicological studies.

The most typical probe molecules used to quantify reactive sites in heterogeneous catalysis are carbon monoxide, for metal NPs,[45] and methanol, for metal oxides, both in the gas/vapor phase. The latter is considered a “smart” probe molecule that can not only quantify the number of surface sites by chemisorption, but also report on their reactive profile by temperature-programmed surface reaction (TPSR), [46,47] a powerful technique to identify and quantify acidic, basic, redox, and bifunctional sites[48,49] on materials that are not thermally sensitive. In addition, several probe molecules in the liquid phase may specifically assess the oxidative potential (OP),[50,51,52,53,54,55] which is particularly relevant to human health due to its involvement in cellular damage by oxidative stress. [10,56,57,58,59,60] Among those, dithiothreitol (DTT) is suggested here as an acellular, liquid-phase, low-temperature probe reaction to assess the nanomaterials OP, as this molecule has been previously used to quantify the oxidative capacity of particulate matter. [61,62,63,64,65,66] We introduce therefore a NAM based on using gas-phase methanol chemisorption and subsequent TPSR as well as liquid-phase DTT consumption in PBS-water solutions with nanomaterials. By normalizing

View Article Online
DOI: 10.1039/D3EN00810J

DTT oxidation rate via methanol chemisorption, we derive the Oxidative Turnover Frequency (OxTOF) to measure surface site reactivity. We suggest dose normalization to the reactive sites' amount and reactivity. As a proof of concept seven metal oxide nanomaterials (CeO_2, ZnO, CuO, Fe_3O_4, Co_3O_4, and two TiO_2 variants), one bimetallic nanooxide ($CuFe_2O_4$) and an oxide with larger particles (Co_3O_4) are analyzed to investigate the usefulness of this NAM to 1), categorize the reactivity of eight benchmark engineered nanomaterials; 2), assess the differences in reactivity between ENMs with the same composition (TiO_2 NM-101 vs TiO_2 DT-51); 3), assess the effect of bimetallic compositions on the surface reactivity of metal nano-oxides (monometallic *vs.* bimetallic); 4), calculate reactive rankings according to three dose metrics based on mass, surface area and surface sites; and 5), assess the size-dependent reactivity of a material, by comparing Co_3O_4 nanoparticles to its larger counterpart.

2 EXPERIMENTAL

2.1 Nanomaterials

All nanomaterials were used as supplied. Two anatase TiO_2 powders were compared: DT51 (CristalACTiV™) and NM-101 (labeled as JRCNM01001a by the supplier, the Joint Research Centre, JRC). In addition, two more JRC samples: CeO_2 NM-211 (JRCNM02101a) and ZnO NM-110 (JRCNM62101a), as well as four commercial samples from Sigma-Aldrich: CuO (ref. number: 544868, CuO-SA), $CuFe_2O_4$ (ref. number: 641723, $CuFe_2O_4$-SA), Fe_3O_4 (ref. number: 637106, Fe_3O_4-SA), and Co_3O_4 (ref. number: 637025, Co_3O_4-SA), were evaluated . **Error! Reference source not found.** summarizes data and information on these proof-of-concept samples. The size dependence of reactivity was evaluated using Co_3O_4 microparticles (ref. number: 221643, Sigma-Aldrich<10 μm).

2.2 Specific surface area

Specific surface area was calculated by the BET method with data obtained in a Micromeritics ASAP 2020 adsorption isotherm equipment. All ENMs were pretreated by degassing under vacuum for 16 h at 120 ºC before nitrogen adsorption at liquid nitrogen temperature.

2.3 Methanol chemisorption and subsequent temperature-programmed surface reaction (TPSR)

View Article Online
DOI: 10.1039/D3EN00810J

Methanol chemisorption/TPSR procedure (see a detailed description in the SI, **Error! Reference source not found.**A and Figure S 2) is made on a clean dehydrated sample. 100-250 mg of nanomaterial (aggregated samples with aggregates ranging from 25 to 100 μm) were diluted with 500 mg of inert SiC (black 180, Navarro SiC S.A.), to ensure isothermal conditions, are and placed in a fixed-bed reactor (0.4 cm internal diameter). The sample is first pretreated by heating from room temperature to 450 ^{0}C at 10 ^{0}C/min in a 150 mL/min synthetic air flow and kept at this temperature for 35 min to ensure the removal of moisture and burn away impurities from its surface. After pretreatment, the sample is cooled down to 100 ºC (or 50ºC for highly reactive ENMs) in synthetic air. After such treatment the surface remains hydroxylated, but not hydrated; next, the flow feed is switched to argon (100 mL/min) purge. The chemisorption temperature was optimized to prevent the formation of multilayers in the case of highly reactive materials, looking for a balance between methanol condensation at lower temperatures and methanol reaction at higher temperatures, either of which would lead to an overestimation of the surface sites.[67,68] After purging, still at 100ºC (or 50ºC for highly reactive ENMs), 100 mL/min of 2000 ppm methanol in argon with 5% helium is fed until saturation, as determined by online mass spectrometry residual gas analysis (cf. supplementary information). The 5%helium in the argon stream is used as an internal reference for online mass spectrometry. The methanol vapor chemisorbs titrating surface hydroxyl groups; this process converts CH_3OH molecule into a chemisorbed CH_3O- moiety, the missing hydrogen atom reacts with the surface hydroxyl thus releasing an H_2O molecule per CH_3OH molecule that chemisorbs. We monitor the effluent gases by a quadrupole residual gas analyzer Pfeiffer OmniStar mass spectrometer. The m/z values followed were: CH_3OH (methanol) = 31, HCHO (formaldehyde) = 30, CH_3OCH_3 (dimethyl ether, DME) = 45, CH_3OOCH (methylformate) = 60, $(CH_3O)_2CH_2$ (dimethoxy methane) = 75, H_2O (water) = 18, and CO_2 (carbon dioxide) = 44. Blank tests were performed with 500 mg of inert SiC (Figure S3). Details on the procedure, the calculation of the reactive surface sites and the surface reactions in methanol-TPSR (equations S1-5) are available in the supplementary material. This methodology is limited to thermally stable samples like metal oxides.

2.4 DTT consumption assay

DDT catalytic oxidation was performed in a batch reactor for 1h. First, a 200 μg/mL suspension of ENM in 1 mM phosphate buffer is obtained by sonication, following

View Article Online
DOI: 10.1039/D3EN00810J

NanoGenoTox SOP (16 min at 400 W and 10% amplitude).[69] 3 mL of the ENM suspension is incubated for 1 h at 37 °C and 500 rpm with 3 mL of 100 µM DTT, obtaining a 6 mL reaction mixture with 100 µg/mL of ENM and 50 µM DTT. Then, the nanoparticles are removed by filtration, and the filtrate, with the unreacted DTT and the reaction products, is mixed with an equal volume of 1 mM Ellman's reagent (5,5′-dithiobis-(2-nitrobenzoic acid), DTNB) to quantify the non-oxidized DTT(**Error! Reference source not found.**B). Ellman's reagent reacts with the thiol groups (-SH) of the free DTT molecules, forming 5-mercapto-2-nitrobenzoic acid, a colorful complex that is measured at 412 nm by UV-Vis spectrophotometry (Shimadzu, UV-2100). In parallel, as a negative control, DTT in phosphate buffer without ENM is incubated under the same conditions and mixed with the Ellman's reagent to evaluate the DTT consumed by direct reaction without catalyst. Hydrogen peroxide 30 % (w/w) in H_2O is used as a positive control, as it provides similar DTT conversion as 1,4-naphthoquinone,[62] being safer and not requiring filtration. All reactions were performed in triplicate. Linearity in measurements at 412 nm of DTT-DTNB nm complex was calibrated (Figure S4). DTT oxidative potential is expressed as DTT conversion (Eq. 1), as a normalized index of oxidant generation using hydrogen peroxide as a positive control (Eq. 2), or as DTT reaction rate, normalized *vs*. mass (Eq. 3), *vs.* ENM surface area (Eq. 4), or *vs.* number of reactive sites (Eq. 5), i.e, OxTOF.

$$\text{DTT depleted (mol \%)} = 100 - \frac{Reaction\ absorbance}{Blank\ absorbance}\cdot 100 \quad \text{(Eq. 1)}$$

$$\text{NIOG (0-1)} = \frac{DTT\ depleted\ by\ nanomaterial}{DTT\ depleted\ by\ positive\ control} \quad \text{(Eq. 2)}$$

$$OP_{mass}\ (mol\cdot s^{-1}\cdot g^{-1}) = \frac{depleted\ DTT\ moles}{time\cdot mass\ of\ NM} \quad \text{(Eq. 3)}$$

$$OP_{area}\ (\mu mol\cdot s^{-1}\cdot m^{-2}) = \frac{depleted\ DTT\ moles}{time\cdot surface\ area\ of\ NM} \quad \text{(Eq. 4)}$$

$$OxTOF\ (s^{-1}) = \frac{depleted\ DTT\ molecules}{time\cdot active\ sites\ of\ NM} \quad \text{(Eq. 5)}$$

2.5 Statistical analysis

DTT OP_{mas}, OP_{area} and OxTOF are expressed as average ± sd (standard deviation). The statistical analysis was performed with SPSS 20 (IBM, Armonk, USA) using logarithmic values to obtain a better normal distribution. One-way ANOVA (Analysis of Variance) was performed to determine statistically significant differences. Subsequently, a Tukey test was

View Article Online
DOI: 10.1039/D3EN00810J

performed to assess pairwise differences with a significance level of $p < 0.05$ and classify ENMs according to the oxidative potential.

3 RESULTS

3.1 Surface area and reactive sites

In the series, TiO_2 NM-101 exhibits the largest BET area, 225 m^2/g; the rest of ENMs have significantly lower BET values: TiO_2-DT51, 84 m^2/g; CeO_2 NM-211, 76 m^2/g; CuO-SA, 12 m^2/g; ZnO NM-110, 9 m^2/g; $CuFe_2O_4$-SA, 33 m^2/g; Fe_3O_4-SA, 11 m^2/g, and Co_3O_4-SA, 26 m^2/g (***Error! Reference source not found.****A*). These data are consistent with the values reported in the literature and in the supplier's technical sheets. [70, 71, 72, 73, 74] ***Error! Reference source not found.****B* illustrates the specific number of sites (mmol per g). While the order of materials remains similar, the relative values change significantly between Figure 2A and B. Thus, the reactive sites surface density (site per nm^2) may follow a different trend. Figure 2C shows this surface descriptor, calculated from **Error! Reference source not found.**A and B data. Interestingly, the ENMs with smaller surface area have higher reactive sites surface density: 16.6 and 21.8 sites/nm^2 for ZnO NM-110 and CuO-SA, respectively (values obtained at 50 ºC). These data show that due to differences in site types and/or distribution, surface area and reactive sites number do not linearly correlate for these samples, as it might be erroneously assumed. It is remarkable that TiO_2-DT51, with 2.7 times lower specific surface area than TiO_2 NM-101, doubles its reactive sites surface density (14 *vs*. 7 sites/nm^2). Therefore, BET (physical) may not be the most relevant descriptor of ENMs surface chemistry. ***Error! Reference source not found.*** *D* summarizes the trends shown in ***Error! Reference source not found.*** *A*-*C*, after data normalization to the most described nanomaterial in the literature: TiO_2 NM-101.

View Article Online
DOI: 10.1039/D3EN00810J

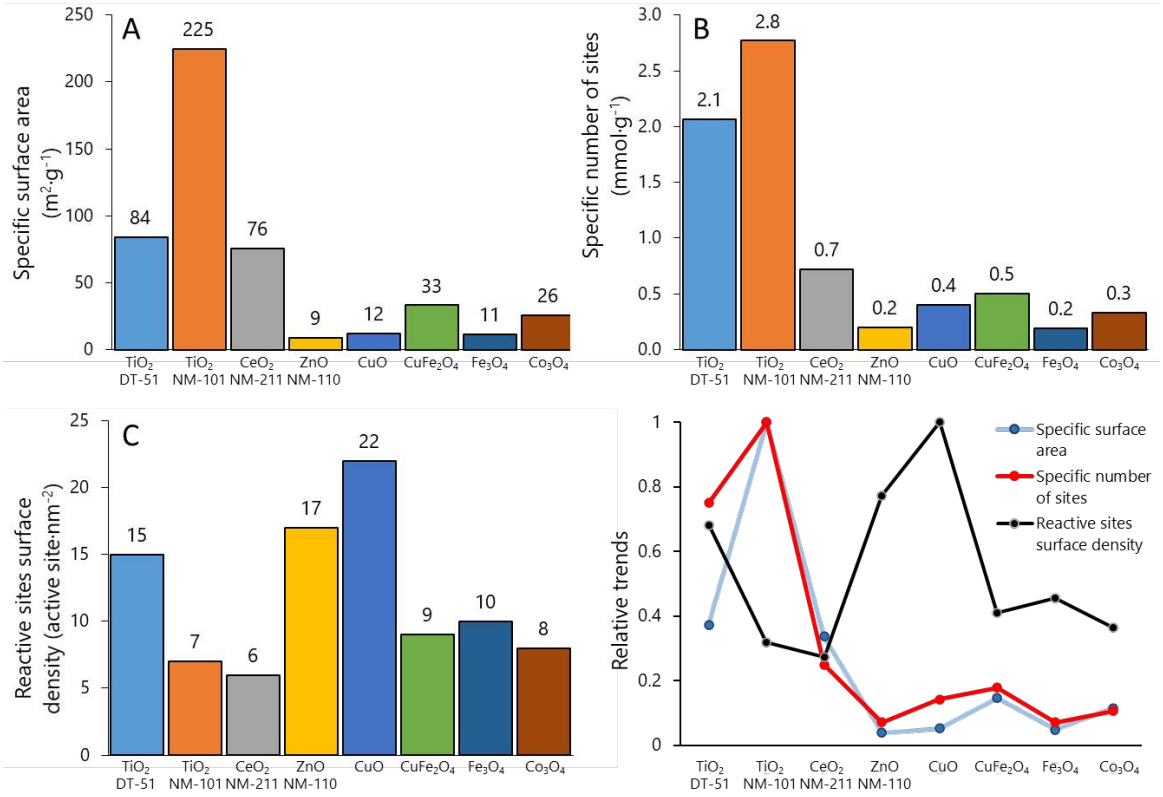

Figure 2. *Surface analysis:* ***A)*** *Specific surface area obtained by N_2 adsorption isotherm,* ***B)*** *Specific number of reactive sites obtained by methanol chemisorption,* ***C)*** *Reactive sites surface density obtained by combination of A and B,* ***D)*** *Comparison of the three surface descriptors (values normalized to the maximum).*

3.2 Reactive profile

The methanol TPSR profiles in **Error! Reference source not found.** provide information on the reactive sites and their reactivity. The typical TPSR products are DME, HCHO and CO_2.

TiO_2 ENMs (DT51 and NM-101) form mainly **dimethyl ether** ***(Error! Reference source not found.*** *A and D),* the characteristic product of acidic reactivity. The maximum production of dimethyl ether occurs at 349 ºC for NM-101 and at 339 ºC for DT51, indicating a weaker acidity of the sites of the latter, which are also fewer, as indicated by the smaller area under the curve. Redox (HCHO) and basic (CO_2) reaction products also form on both titania samples. The redox site is active in a broad temperature range, which indicates a broad

View Article Online
DOI: 10.1039/D3EN00810J

distribution of oxidation reactivities, and that the oxidation capacity is moderate, since rather high temperatures are required to express it.

Oxidative sites produce **HCHO**. Thus, CeO_2 exhibits redox sites where methanol is oxidized to formaldehyde, with a maximum near 259 ºC (***Error! Reference source not found.****G)*; ceria oxidative sites exhibit a narrower peak, which indicates that most oxidizing sites have similar reactivity. This is unlike the broad distribution of oxidative site types on the titanias, in the 150 to 400 ºC range. Moreover, ceria has a higher oxidation capacity, for its maximum is at a lower temperature than the average of HCHO formation on the titania samples.

ZnO NM-110, $CuFe_2O_4$-SA, Fe_3O_4-SA, Co_3O_4-SA and CuO-SA (***Error! Reference source not found.*** *C-H*) produce mainly **CO_2**, but the temperatures at which CO_2 reaches a maximum differs significantly, for some it is near 220-250ºC, and for others above 300ºC. The significantly higher maximum temperature for CO_2 production is indicative of basic materials, where methoxy species adsorb strongly and can only desorb at very high temperatures, thus being combusted (ZnO NM-110 and Fe_3O_4-SA). Instead, the easier formation of CO_2 (some 100 ºC lower temperatures) is indicative of a high oxidation capacity, leading to total oxidation CO_2 rather than to partial oxidation formaldehyde (CuO-SA, $CuFe_2O_4$-SA and Co_3O_4-SA).[49] Evaluated as a reference, micrometric Co_3O_4 (Figure S5) showed a similar reactive profile than Co_3O_4 nanoparticles. Thus, the nature of the surface sites in nano and micro CuO remains essentially alike, with the critical difference that a minimum part of the reactive sites is exposed in the larger CuO particles, hence the risk of exposure to larger CuO particles is minimized. In summary, *methanol TPSR reactive profiles may classify materials based on a linear combination of their acidic/basic reactive profile vs. its oxidation profile* (**Error! Reference source not found.***I*). In this categorization, the X-axis qualitatively indicates how oxidizing the material is, while the Y-axis moves from acidic to basic character. Thus, TiO_2 DT51 and NM-101, ZnO NM-110, and Fe_2O_3-SA have a moderate oxidation capacity, being Fe_2O_3-SA and ZnO NM-110 more basic and both TiO_2 more acidic. On the other hand, CeO_2 NM-211, Co_3O_4-SA exhibit increased oxidation capacity, and the highest is for CuO-SA and $CuFe_2O_4$-SA.

View Article Online
DOI: 10.1039/D3EN00810J

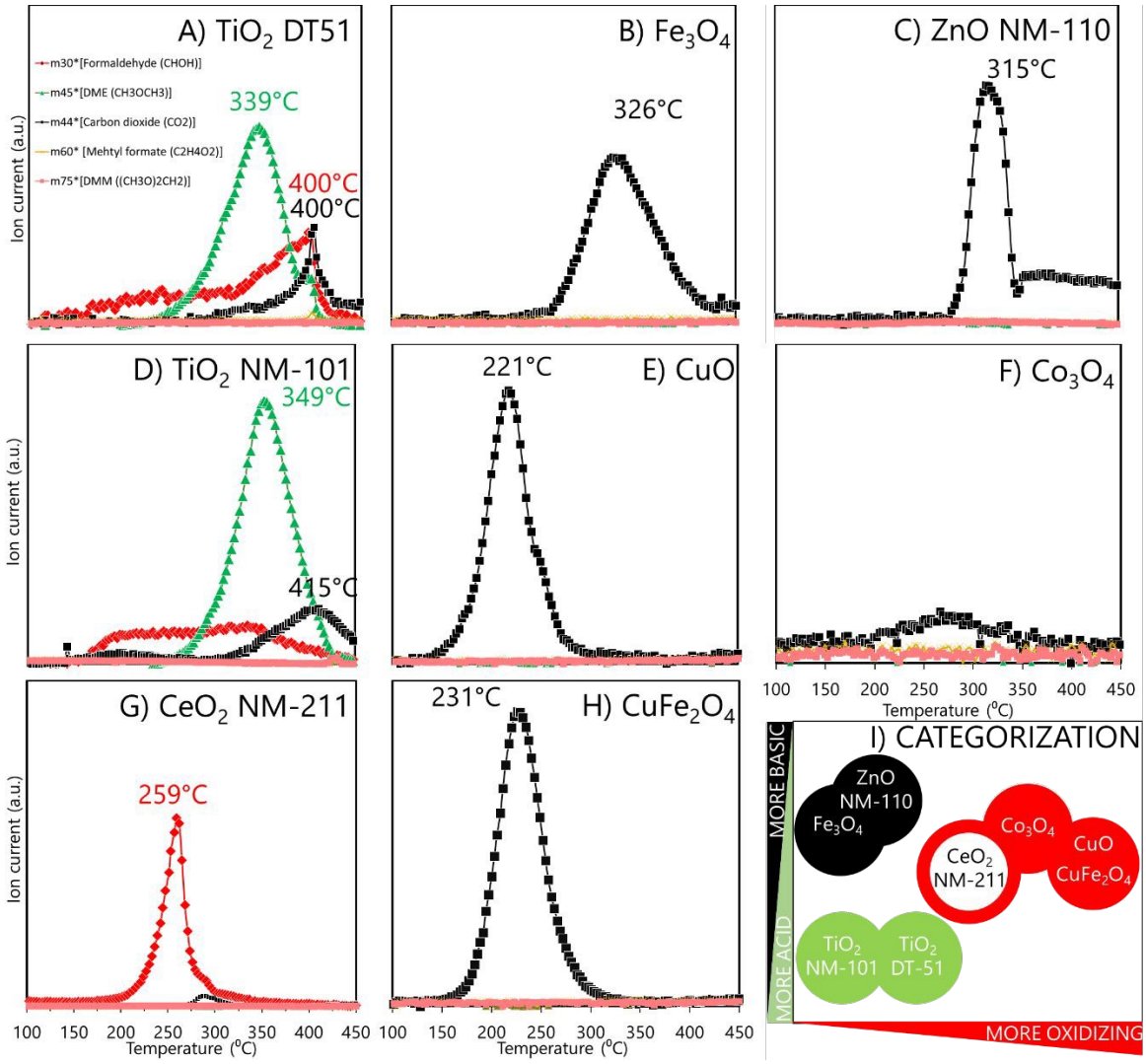

Figure 3. *Temperature-programmed surface reaction products of pre-adsorbed methanol analysed by mass spectroscopy for two different anatase TiO_2: DT51 (A) and NM-101 (D), for Fe_3O_4-SA (B), for ZnO NM-110 (C), for CuO-SA (E), for Co_3O_4-SA (F) for CeO_2 NM-211 (G), and for $CuFe_2O_4$-SA (H). Formaldehyde signal (red) is obtained for redox sites, dimethyl ether signal (green) for acid sites, and carbon dioxide (black) for basic or high reactive redox sites. ENMs classification by MeOH-TPSR results is shown in I) with the same colour code. For a given colour, filled circles are more reactive than empty circles.*

3.3 Oxidative potential

Error! Reference source not found. illustrates DDT catalytic oxidation results for 1h reaction, normalized vs. different descriptors; the corresponding classification of the ENMs based on Tukey's test using the logarithm of OP_{mass}, OP_{area} and OxTOF are provided on the right side of the plots. ZnO NM-110 was not included in the analysis because it dissolves in

View Article Online
DOI: 10.1039/D3EN00810J

the reaction media and Zn cations get complexed by DTT,[66] so no free and uncomplexed DTT is available for interaction with the ZnO NM-110 surface, and thus the results are close to the negative control.[66] The relative oxidative potential of the other ENMs significantly depends on the descriptor. The positive control normalization has little impact on the relative conversion trend (*Figure S6*), which is similar to that of the specific reaction rate shown in ***Error! Reference source not found.*** *A*: CuO-SA ≈ $CuFe_2O_4$-SA >>> Co_3O_4-SA ≈ TiO_2 NM-DT-51 ≈ TiO_2 NM-101 ≈ CeO_2 NM-211 > Fe_3O_4-SA; according to Tukey's test, only CuO-SA and $CuFe_2O_4$-SA are classified as significantly highly reactive ENMs. The differences between these ENMs' reactivities are clearly amplified when the oxidation rate is normalized to the ENM surface area (**Error! Reference source not found.**B), which underlines that CuO-SA surface, being small (**Error! Reference source not found.**A), is significantly more reactive that other ENMs' surfaces in the series. Actually, Tukey's test reveals three reactivity groups of ENMs according to OP_{area} descriptor: CuO-SA > Co_3O_4-SA ≈ $CuFe_2O_4$-SA > TiO_2 DT-51 ≈ CeO_2 NM-211 ≈ TiO_2 NM-101 ≈ Fe_3O_4-SA. *Mass or BET normalizations cannot tell how reactive each site is, so this trend stands on assuming that all physical areas are equally populated by equally reactive sites, which is not the case.* Normalization per reactive site (**Error! Reference source not found.**C) delivers the OxTOF, which shows that CuO-SA and $CuFe_2O_4$-SA sites are the most oxidizing ones, followed by Co_3O_4-SA, and ca. fourfold more reactive than ceria sites. The remaining group of materials exhibit significantly lower oxidation activity, according to Tukey's test: CeO_2 NM-211 > TiO_2 DT-51 ≈ TiO_2 NM-101 ≈ Fe_3O_4-SA. A larger amount of sites can make up for individual site lower reactivity; therefore, both pieces of reactivity information, global (per material dose) and individual (per site), are important to understand and classify ENMs. Among these descriptors, only OxTOF can identify with statistical significance that ceria has more reactive redox sites than titania ENMs. *From a chemical perspective, turnover frequency values may allow a better quantitative comparison of oxidative potential and provide a more accurate insight into reactivity at a molecular scale.*

View Article Online
DOI: 10.1039/D3EN00810J

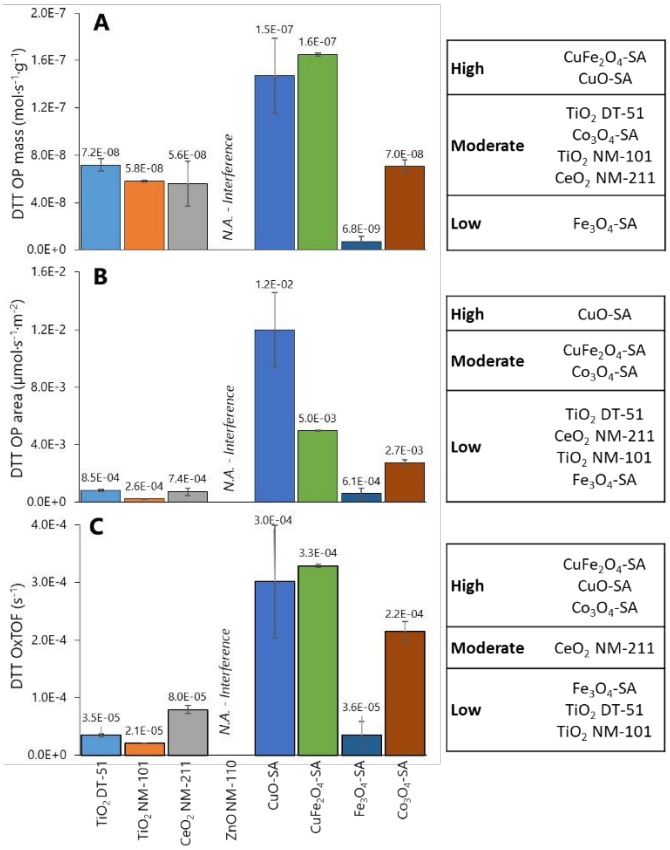

***Figure 4**. Oxidative potential evaluated by DTT assay and expressed as: reaction rate per mass (A), reaction rate per surface (B), oxidative turnover frequency (reaction rate per reactive site) (C). Left: Averaged OP values (n=3) with error bars indicating the standard deviation. Right: Statistical analysis for classification of the ENMs by OP based on Tukey' test comparison.*

Size dependence of reactivity was evidenced via comparison of Co_3O_4 nanoparticles *vs* microparticles, which exhibited a DTT depletion of 6.7 ± 4.2% of DTT depletion, equivalent to a NIOG of 0.08 ± 0.04, that is, around 7 times lower oxidative capacity than its nanoparticle counterpart. This is essentially due to the significantly smaller fraction of reactive sites that are exposed.

3.4 Dose metrics applied to bibliographic toxicological data

Bibliographic toxicity information for TiO_2 NM-101, CeO_2 NM-211, ZnO NM-110, CuO-SA, Fe_3O_4, $CuFe_2O_4$ and Co_3O_4 was extracted from eNanoMapper[75,76] and the literature to

View Article Online
DOI: 10.1039/D3EN00810J

investigate possible correlations of the surface reactivity with in vitro toxicity descriptors (**Error! Reference source not found.**).

CuO-SA is highly toxic to pulmonary cells, causing cell death and impairing cell functions after 24-hour exposure. [77] The mechanism involves ion release, autophagy activation, and increased lipid peroxidation. [78] [79] [80] Animal models support its lung inflammatory effects but do not show teratogenic potential. [81] [82] In terms of dose metrics, this ENM, the most oxidant in the series, exhibits significant effects on A549 cell viability at 5, 10 and 17.75 µg/mL gravimetric doses, equivalent to 2, 4 and 7.1 µmol/L sites doses, in different studies. [78]

$CuFe_2O_4$-SA cytotoxic effects on human lung (A549) and liver (HepG2) cells were analyzed, illustrating a dose-dependent toxicity within a concentration range of 10–100 µg/ml (*i.e.*, 5-50 µmol site/L). Key observations include mitochondrial membrane potential (MMP) depletion, upregulation of the caspase-3 gene, and increased caspase-3 enzyme activity, suggesting apoptotic cell death as a consequence of exposure to these ENM. Furthermore, an imbalance in cellular redox status was evident through the induction of ROS and depletion of glutathione (GSH), indicating oxidative stress as a potential underlying mechanism of cytotoxicity.[83]

ZnO NM-110, extensively studied in vitro, exhibits adverse effects in multiple cell lines, with immune system alterations observed in Raw 264.7 and MH-S macrophages (EC50: 10-25 µg/mL, i.e., 3-7.5 µmol/L sites doses), pulmonary cell lines displaying cytotoxic and genotoxic effects (LC50: 76 µg/mL, that is, 22.8 µmol sites/L), [84] [85] and respiratory and male reproductive cell lines affected (EC50 < 20 µg/mL, so less than 6 µmol sites/L).[86] Hepatic damage in C3A was evidenced by WST-1 test.[87] Proteomic analysis in NRK-52E reveals pronounced effects, particularly in actin carbonylation; this ENM is classified as highly cytotoxic and a protein carbonylation agent.[88] Caco-2 cell lines exhibit cytotoxicity due to dissolved Zn^{2+}, and HUVEC cell lines show reduced mitochondrial viability attributed to intracellular Zn ions and ROS. In contrast, TiO_2 NM-101 shows no cytotoxicity or inflammatory markers. [89] [90]

TiO_2 NM-101 exhibited no significant cytotoxicity in A549, HepG2, HK-2, and C3A cell lines. However, C3A cells showed IL-8 release, indicating inflammation. [87,91] BEAS-2B cell viability

View Article Online
DOI: 10.1039/D3EN00810J

was unaffected by TiO_2 at concentrations of 1-100 μg/mL, i.e., 2.8-280 μmol sites/L, but DNA damage and IL-6 release were observed at 10 (28 μmol sites/L) and 100 μg/mL , respectively. RAW 264.7 macrophages exposed to TiO_2 NM-101 released IL-6 and TNF-α at higher concentrations (100 μg/mL). [92]

The toxic mechanism of **CeO_2 NM-211** remains unclear, but protein aggregation and fibrillation are proposed hypotheses. [93, 94] CeO_2 NM-211 induced moderate pro-inflammatory cytokine release in rat precision-cut lung slices (PCLuS) at 100 μg/mL, which represents a sites concentration of 70 μmol/L. It is in line with other In vivo studies, where inflammatory markers increased in the bronchoalveolar lavage fluid (BALF) after 14 days of exposure.[95,96] In vitro, A549 cells exposed to similar cerium oxide nanoparticles at concentrations up to 100 μg/mL showed no cytotoxicity. [97] In contrast, NR8383 alveolar macrophages exhibited cytotoxicity at 90 μg/mL (63 μmol site/L) along with signs of inflammation, including TNF-α release, after CeO_2 NM-211 exposure. [98] These results will be analyzed in section 4.2 with respect to our in chemico method, as gravimetric, surface, and reactive site-based concentrations offer insights into the diverse doses of ENMs in toxicology.

Fe_3O_4-SA showed no adverse effects on A549 cell viability for 24-72 h for concentrations up to 100 μg/mL (equivalent to 20 μmol site/L), even after being internalized within the cells following 12 h exposure. Furthermore, an increase in lysosomal activity was not detected after 6 h. However, a concentration-dependent decrease in mitochondrial membrane potential at 100 μg/mL was statistically significant. There was no induction of pro-inflammatory cytokine secretion, including IL-1β, IL-6, IL-8, and TNF-α. This evidence suggests that iron oxide exhibits low cytotoxicity.[99]

Cyto-genotoxic and inflammatory responses of **Co_3O_4-SA** in human alveolar (A549) and bronchial (BEAS-2B) cell lines was evaluated at concentrations ranging from 1–40 μg/ml, equivalent to 0.3-12 μmol site/L. Notably, A549 cells exhibited no cytotoxicity, while BEAS-2B cells showed reduced viability at 40 μg/ml and early membrane damage at 1, 5, and 40 μg/ml. Significant direct and oxidative DNA damage was observed in A549 cells at 20 and 40 μg/ml, with no impact on cytokine release. Conversely, BEAS-2B cells exhibited significant direct DNA damage at 40 μg/ml and notable oxidative DNA damage at lower concentrations, coupled with increased TNF-α and IL-8 release at specific concentrations

View Article Online
DOI: 10.1039/D3EN00810J

and exposure times. These results underline the differential cellular responses to cobalt oxide nanoparticles, highlighting the enhanced sensitivity of BEAS-2B cells to cytotoxic, genotoxic, and pro-inflammatory effects.[100] The genotoxic effects of cobalt oxide in Chinese hamster lung fibroblast (V79) cells, primarily mediated by reactive oxygen species, were used to compare with the bulk counterparts: Co_3O_4-SA nanoparticles exhibit pronounced genotoxic effects compared to bulk Co_3O_4 macroparticles, due to significant cytotoxicity and DNA damage, attributed to enhanced ROS generation. The mitigation of genotoxic effects with N-acetylcysteine, a ROS scavenger, further confirms the central role of ROS in nanoparticle-induced toxicity. The nano-sized particles facilitate closer cellular interactions, leading to significant cytotoxicity and DNA damage from ROS, unlike the minimal interaction and impact observed with bulk materials.[101]

4 DISCUSSION

4.1 ENMs' surface sites and reactivity

The exponential increase in surface-to-volume ratio as particle size decreases to a few nanometers is crucial; additionally, quantum confinement and discrete energy levels alter electronic states and surface reactivity. We focus on the phenomenological consequences of this, not its origins. A comprehensive categorization of ENM requires an understanding of their reactivity characteristics; namely, the number of reactive surface sites, their reactive nature and relative reactivity. Nanomaterials can oxidize molecules directly or generate ROS through interactions with biological systems, which may also alter their properties. These interactions depend on the surface properties of the nanomaterials, including reactive sites beyond physical surface area. While oxidative potential is often highlighted, acidic and basic sites also significantly impact molecular interactions. Our method maps all reactive sites to provide a comprehensive description of nanomaterials and enable more reliable grouping based on their chemical surfaces. According to our data, reactivity-triggered nanotoxicity not only depends on the number and reactivity of redox sites but also on sites of basic and acidic nature. Their interplay determines how ENM's interact with the environment and with our physiology. Parameters like site-specific numbers and TOF (*e.g.*, DTT OxTOF) are essential in elucidating the reactive potential of ENMs and linking them to potential adverse effects. Additionally, TPSR profiles provide insights into these sites' relative presence and reactivity, influencing toxicity profiles. OxTOF tendency in Figure 4C shows CuO-SA ≈ $CuFe_2O_4$-SA > Co_3O_4-SA >> Ce_2O_3 NM-211, in line with oxidation capacity assessed by methanol-TPSR;

View Article Online
DOI: 10.1039/D3EN00810J

also following this correlation, the titanias, Fe_3O_4-SA and ZnO NM-110 exhibit very little methanol oxidation. Therefore, DTT probe reaction is an oxidative dehydrogenation forming a disulfide group that appears to run mechanistically parallel to the oxidative dehydrogenation of methanol to formaldehyde in TPSR experiments. The use of chemisorption avoids interference from ion release, buffer reactivity (as observed with some probe reactions in phosphate medium), [102] or agglomeration that would take place in liquid-phase assays.

Reactive site surface density quantified by methanol chemisorption in our series is consistent with values reported in the literature for oxide ENMs, ranging between 0.4 and 22 sites/nm^2, but typically up to ca. 7 sites/nm^2, corresponding to a monolayer.[39] The high number of reactive sites on CuO-SA (22) and ZnO NM-110 (17) surfaces must be related to a highly reactive interaction with chemisorbed methoxy groups. Multilayer formation is likely on ZnO NM-110 basic sites, as suggested for La_2O_3, MgO or Cr_2O_3,[39] whereas CuO-SA is a highly oxidizing material that transforms surface methoxy groups into formate groups[103,104,105]. This is consistent with the extensive CO_2 desorption profile during MeOH-TPSR. Hence, the chemisorption temperature was set to 50 ºC is these materials. CO_2 formation at low temperatures on highly reactive CuO-SA is characteristic of formates decomposition, while the formation of CO_2 at high temperatures on the alkaline ZnO NM-110 is associated with the decomposition of carbonates.[104] The determination of reactive sites provides complementary insight to ROS determination probes, which sensitivity depends on different features. For instance, the basic character of ZnO NM-110 and its high reactive site surface density correlates with the ferric reduction ability of serum (FRAS) assay, an indirect measurement of ROS by total antioxidant depletion, and protein carbonylation assay.[106] In another study, electron spin resonance (ESR) spectroscopy with 3-carboxy- 2,2,5,5-tetramethylpyrrolidine 1-oxyl (CPH) and 5,5-dimethyl-1-pyrroline N-oxide (DMPO) probe molecules quantifies the oxidative potential of ENMs by determining the ROS production.[107] Less ROS were produced by CeO_2 NM-211 and ZnO NM-110 when compared with CuO,[106] which agrees with our reactive ranking based in OxTOF data, and the higher number of reactive surface sites of the latter; the CPH spin probe (more sensitive to singlet oxygen, superoxide radicals, and peroxynitrites) revealed higher ROS production by ceria than by zinc oxide, whereas the DMPO spin trap (more sensitive to hydroxyls and superoxide radicals) showed the opposite trend. Raman spectroscopy, which is highly

View Article Online
DOI: 10.1039/D3EN00810J

sensitive to peroxide-related species, can be used to further analyze this. *In situ*[108,109] and *operando*[110] Raman spectra show that superoxide and peroxide species are generated at the surface of different ceria materials by interaction with molecular oxygen, but there are no reports of superoxide species formed at the surface of ZnO and TiO_2. Thus, reactive superoxide species would only account for DMPO and CPH by CeO_2 NM-211, but not by ZnO NM-110 or titania; therefore, ZnO NM-110 must generate more hydroxyls than CeO_2 NM-211 to account for the DMPO probe results.

Titania, the least-reactive material in our series, highlights the complexity of categorizing nanomaterials. Even with the same composition (TiO_2) and crystalline phase (anatase), titania samples differ significantly in BET surface area, reactive site density, and strength.TiO_2 NM-101, as measured by terephthalic acid assay, generates ROS upon photoirradiation, but not in the dark.[111] Conversely, ROS generation detected via DMPO trap was significantly higher than the control not only upon irradiation, but also in the dark - although to a lesser extent.[111] Several studies on titania reactivity and photoreactivity highlight the impact of species in biological systems (e.g., carboxylic acids, amines) that strongly adsorb onto titania surfaces, affecting reactivity.[102 ,112]. This underscores the importance of characterizing all surface reactive sites: acidic, basic, and redox. The band gap of metal nano-oxides, crucial for correlating with oxidative stress and pulmonary inflammation from photocatalytic ENMs, strongly depends on particle size, nuclearity, and the nature of nearby elements, serving as an indicator of increasing quantum effects.[113–115]

The strong influence of the titania structural variety on its surface reactivity is being described from the perspective of nanoinformatics,[116,117] which uses computational approaches to understand the surface structure and reactivity of ENMs, using this data in a FAIR (Findability, Accessibility, Interoperability and Reusability) implementation for the nanosafety community.[118,119]

4.2 Oxidative surface sites and *in vitro* cell viability

As in vitro assays monitor different effects (cell viability, protein release, inflammation, etc.) in specific cell lines (A549, dTHP-1, etc.) and do not provide information about biodistribution, biopersistency or biotransformation[23] of nanomaterials, they are limited in

View Article Online
DOI: 10.1039/D3EN00810J

predicting the overall toxicological profile, comparisons are not straightforward, and correlations with physicochemical properties of ENMs can only be done as a first approximation. [77,120]The *in vitro* toxic effects of ENMs that over-oxidize methanol to CO_2 in TPSR and show redox surface reactivity (Co_3O_4-SA, $CuFe_2O_4$-SA and CuO-SA) significantly affected different cell lines,[83,101,120] underscoring the implication of reactive surface sites in nanotoxicity field. When comparing CuO-SA and ZnO NM-110, the higher reactive sites surface density and the lower temperature of maximum methanol conversion to CO_2 of the former are indicative of a higher reactivity of CuO-SA, which correlates with the higher toxicity reported by cell viability assays with A549 line: EC_{50} for 24 h exposure was 17.75 for CuO-SA and 76 µg/mL for ZnO NM-110.[84,120] Site-based dose metrics underlines the higher *in vitro* toxicity of CuO-SA sites. DTT OxTOF could not be evaluated for ZnO NM-110; still, the physical-chemical properties reported in the literature -oxidation number, ionic potential, surface reducibility and redox reactivity- are consistent with its high *in vitro* toxicity.[121] Nevertheless, ZnO NM-110 is a complex ENM, because its surface reactivity has biocidal properties,[122] but its mode of action is essentially by dissolution.[121]

CuO-SA has the highest reactive sites surface density in the series, though not the most sites per gram, and shows the highest OxTOF (Figure 2D, Figure 4E) along with $CuFe_2O_4$-SA. This correlates with their inflammatory effects, commonly associated with ROS generation and oxidative stress, making these ENMs the most toxic in the series.[123] CuO-SA's oxidative damage was evaluated in HepG2 cells, with endocytosis transporting nanoparticles to endo/lysosomes, leading to lysosome disruption and copper ion overload.[124] This mechanism may involve surface reactivity, initially overlooked due to lack of information on reactive sites. CuO-SA induced oxidative changes in A549 cells, increasing protein carbonylation, oxidizing protein thiols, and decreasing cell viability, with no effects from dissolved copper ions.[125] These effects were more pronounced in CuO-SA with higher crystalline defects and ROS production, likely due to higher reactive sites surface density. [125] Other studies reported CuO-SA's distinct cytotoxicity in A549 and HeLa S3 cells from direct interactions with cellular components, facilitated by greater surface area and reactive sites density compared to microparticles. This parameter could facilitate the surface interactions of CuO-SA with their surroundings. For that reason, elevated intracellular levels can disrupt copper homeostasis, leading to pro-oxidative reactions[126] produced at the surface of CuO-SA nanoparticles.[127]

View Article Online
DOI: 10.1039/D3EN00810J

Co_3O_4-SA nanoparticles exhibited higher reactivity for DTT depletion than bulk material, reflected in genotoxic effects V79 cells, primarily mediated by reactive oxygen species. This indicates that nano-sized Co_3O_4-SA induces significant cytotoxicity and DNA damage, unlike larger particles. [101] The toxicity of TiO_2 NM-101 is not fully understood due to inconsistent evidence across different tests.

In the case of CeO_2, the literature has typically linked its toxicity with reactive oxygen species generation and the Ce^{3+}/Ce^{4+} ratio,[128] related to the exposed phase of ceria [129,130] and its defects, which is also key for catalytic activity.[108] These properties can be easily determined by several techniques[131–135] CeO_2 NM-211, with redox surface sites and moderate oxidative capacity, causes cell death by apoptosis and DNA damage in pulmonary cell lines.[136,137] The OxTOF of CeO_2 NM-211 is between those of the titania ENMs and of CuO-SA, despite its low BET. This is consistent with the intense formaldehyde production in MeOH-TPSR, maximum at 259 ºC, and with characterization reported in the literature: CeO_2 NM-211 surface contains 22% Ce (III) (XPS), indicative of redox sites, which induce ROS generation, as detected by ESR. [131–135] CeO_2 is highly oxidizing, while defect-rich CeO_{2-x} has antioxidant properties. This versatility is used to engineer ceria nanoparticles by tuning its properties.[138,139] and, thus, its performance e.g. in catalysis, from combustion to selective oxidation[131,140,141], and in biomedical applications, from biocidal to antioxidant [138,139,142]. The dynamic states of ceria nanomaterials in aqueous media[143] or biological media[132,144,145] resulting in defective ceria are extensively investigated[146].

ZnO NM-110, which induces protein carbonylation,[147] has high reactive site surface density, facilitating the formation of a protein corona. This aligns with reports on BSA-ZnO interactions, which demonstrate that protein adsorption on ZnO NM-110 surface is higher compared to other ENMs like TiO_2 NM-110.[84] Despite TiO_2 NM-110 having a larger surface area, its reactive sites surface density is lower than that of ZnO NM-110.

Titania and iron oxide exhibit the lowest reactivity. Fe_3O_4-SA showed no adverse effects even after being internalized within the cells following 12 h exposure. Similarly, both titania samples convert methanol into carbon dioxide, but above 400 ºC and to a limited extent, as they are essentially acidic. This low redox reactivity is consistent with their low DTT OxTOF.

View Article Online
DOI: 10.1039/D3EN00810J

In line with our hypothesis, the high BET area of TiO_2 NM-101 does not directly correlate with adverse effects. While it has a high surface area (a physical feature) its chemical reactive profile counterpart does not run in parallel. The number of surface reactive sites is low, and their reactivity is moderate. TiO_2 NM-101 is a relatively safe ENM, with no cytotoxicity for cell viability in immune, hepatic, reproductive and pulmonary cell lines such as A549, HepG2, HK-2 or C3A. There are no toxicological data for TiO_2-DT51, but the lower number and reactivity of its sites predicts that DT51 would be safer than NM-101. Fe_3O_4, classified as low redox reactive via DTT OxTOF, is described as a safe ENM in terms of *in vitro* evaluation in the literature.[99]

An *in chemico* classification of ENMs can thus be proposed based on methanol chemisorption, reactivity of surface sites and DTT Oxidative Turnover Frequency that may correlate with *in vitro* toxicity sites-based dose metrics: *CuO-SA ≈ $CuFe_2O_4$-SA > Co_3O_4-SA ≈ ZnO NM-110 >> CeO_2 NM-211 ≥ Fe_3O_4-SA ≈ TiO_2 NM-110*

4.3 Reactive surface site-based dose metrics

Recently, some works emphasized the critical importance of adopting dose metrics that reflect the relevance of surface and particle number when assessing the nanotoxicity of ENMs, as traditional mass-based dose metrics are insufficient for evaluating the unique toxicological responses of nanoscale particles.[148,149] These studies collectively underscore the need for more accurate dose metrics to assess the potential risks associated with ENMs. Due to the assumption that not all physical areas are equally populated by equally reactive sites, the reactive sites concentration is proposed as a tool to better quantify the ENMs exposition. For example, TiO_2 NM-101 has 4 times higher specific number of reactive sites than CeO_2 NM-211 (2.8 vs 0.7 mmol/g), but also 3 times higher surface area, so the reactive sites surface density is only slightly higher for the titania (7 vs. 6 sites/nm^2), and therefore the comparison is similar by DTT OxTOF and by OP_{area}: TiO_2 NM-101 has 3-4 times less oxidative potential than CeO_2 NM-211. A different impression is provided by OP_{mass}. Hence, while mass or physical surface area do not provide a site-relevant dose metrics, the number of reactive sites connects with reactivity-triggered effects. This may serve as a new possible dose metrics as an approach to assess the exposure to nanomaterials. The differences are greater when TiO_2 NM-101 is compared to CuO-SA, with very low specific surface area, and thus high reactive sites surface density. These are much more reactive than those of titania

View Article Online
DOI: 10.1039/D3EN00810J

and ceria, as observed by DTT OxTOF; but not as much as OP_{area} indicates. Moreover, a dose metrics based on reactive sites underscores that CuO-SA, with a dose of sites of 4 μmol/L, is capable of producing a significant adverse effect in A549, while 280 μmol/L of titania sites did not significantly decrease cell viability.

5 CONCLUSIONS AND OUTLOOK

Reactive-based nanotoxicity is primarily governed by the surface chemistry of engineered nanomaterials, making catalysis science principles highly relevant to describing the reactive nature of ENMs. Our findings conclude that 1) The specific surface area does not reliably correlate with nanomaterial reactivity, necessitating consideration of surface sites quantity, nature, and reactivity for categorization and site-specific dosing; 2) this can be achieved by a new approach methodology that quantifies and describes reactive surface sites by chemisorption and reaction tests with probe molecules. 3) Methanol offers a triple benefit: it quantifies surface sites through chemisorption, characterizes surface reactivity (acidic, basic, or redox) via temperature-programmed surface reaction, and overcomes limitations of liquid-phase reactions, such as possible ion release, pH-dependent agglomeration, effects of the dispersion protocol, or stability issues, providing insights into the primary reactivity of thermally-stable nanomaterials such as metal oxides. 4) Combining site quantification with physiologically relevant oxidation reactions, like DTT, allows for calculating site-specific oxidative reactivity (OxTOF), aiding nanomaterial classification: CuO-SA, $CuFe_2O_4$-SA, Co_3O_4-SA are the most oxidizing ENMs, according to a higher *in vitro* toxicity, while less reactive ENMs does not produce adverse effects in *in vitro* models.

CuO-SA, $CuFe_2O_4$-SA, Co_3O_4-SA, Fe_3O_4-SA, ZnO NM-110, CeO_2 NM-211 and two TiO_2 ENMs (DT51 and NM-101) are ranked into three categories with statistically different reactivity based on DTT. This fundamental site-specific reactivity information is a relevant descriptor to group ENMs and, ultimately, understand nanotoxicity. Moreover, the behavior of a given material not only depends on its specific nanoform (e.g., crystallinity, size, band gap, solubility, hydrophobicity, surface charge, aspect ratio or shape), but also on its chemical reactive features, like the number of surface reactive sites, their nature, their reactivity and their relative populations. In another cases, the adverse effect would not appear related to the reactivity but to other features, like in multiwalled carbon nanotubes.[150]

View Article Online
DOI: 10.1039/D3EN00810J

This new methodology offers a complementary *in chemico* approach to unravel nanomaterial modes of action. To validate its effectiveness, further testing with additional reference and real-life ENMs and relevant and comparable toxicity information is essential. On a broader vista, the correlation with cellular assays will help establish molecular insight into the reactive basis of nanotoxicity. There are, however, significant structure, reactivity and toxicity data gaps to connect adverse effects with chemical reactivity. This approach aims to elucidate the specific pathways impacted by ENMs, highlighting their role in achieving a comprehensive understanding of nanomaterial toxicity and advocating for safe-by-design principles. Filling these data gaps is in the mission of nanoinformatics and nanosafety projects, supported by platforms like eNanoMapper. Mapping all reactive properties enables a more relevant grouping of nanomaterials since the acidic, basic and redox properties not only reflect their reactivity for adverse effects but also for interaction with species and molecules in biological systems.

6 ACKNOWLEDGMENTS

The authors acknowledge the financial support by the European Commission H2020 project NanoInformaTIX (GA 81446). JRC reference materials were supplied by Dr. Juan Riego Sintes at JRC-Ispra.

7 AUTHOR CONTRIBUTIONS

M. A. Bañares: Conceptualization, original idea, supervision, writing-original draft preparation; V. Alcolea-Rodriguez.: data curation, writing-original draft preparation, investigation, statistical analysis, experimental methodology; R. Portela: Analysis, planning, supervision, writing-original draft preparation. V. Calvino-Casilda: reviewing and editing

All authors equally contributed to the writing.

8 AUTHORS' FULL NAME, ORCID, E-MAIL, CONTRIBUTIONS:

1. V. Alcolea-Rodriguez https://orcid.org/0000-0002-2392-0817 victor.alcolea@csic.es
2. Raquel Portela: http://orcid.org/0000-0002-1882-4759 raquel.portela@csic.es
3. Miguel A. Bañares: http://orcid.org/0000-0003-3875-4468 miguel.banares@csic.es
4. V. Calvino-Casilda https://orcid.org/0000-0002-2756-2164 vcalvino@ieec.uned.es

View Article Online
DOI: 10.1039/D3EN00810J

All authors have given approval to the final version of the manuscript. The authors declare no competing financial interest.

9 REFERENCES

1 Serrano-Lotina A, Portela R, Baeza P, Alcolea-Rodriguez V, Villarroel M, Ávila P. Zeta potential as a tool for functional materials development. *Catal Today* 2022. doi:10.1016/j.cattod.2022.08.004.

2 Pacchioni G. Oxygen Vacancy: The Invisible Agent on Oxide Surfaces. *ChemPhysChem* 2003; **4**: 1041–1047.

3 European Commission, Joint Research Centre, Rauscher H, Kestens V, Rasmussen K, Linsinger T, Stefaniak E. Guidance on the implementation of the Commission Recommendation 2022/C 229/01 on the definition of nanomaterial. *Publications Office of the European Union* 2023. doi:10.2760/237496.

4 Kasemets K, Ivask A, Dubourguier HC, Kahru A. Toxicity of nanoparticles of ZnO, CuO and TiO2 to yeast Saccharomyces cerevisiae. *Toxicology in Vitro* 2009; **23**: 1116–1122.

5 Nel A, Xia T, Mädler L, Li N. Toxic Potential of Materials at the Nanolevel. *Science (1979)* 2006; **311**: 622–627.

6 Buzea C, Pacheco II, Robbie K. Nanomaterials and nanoparticles: Sources and toxicity. *Biointerphases* 2007; **2**: MR17–MR71.

7 Talebian S, Rodrigues T, Das Neves J, Sarmento B, Langer R, Conde J. Facts and Figures on Materials Science and Nanotechnology Progress and Investment. *ACS Nano* 2021; **15**: 15940–15952.

8 Khan I, Saeed K, Khan I. Nanoparticles: Properties, applications and toxicities. *Arabian Journal of Chemistry* 2017. doi:10.1016/j.arabjc.2017.05.011.

9 Kinnear C, Moore TL, Rodriguez-Lorenzo L, Rothen-Rutishauser B, Petri-Fink A. Form Follows Function: Nanoparticle Shape and Its Implications for Nanomedicine. *Chem Rev* 2017; **117**: 11476–11521.

10 Haase, A. & Klaessig, F., (2018). EU US Roadmap Nanoinformatics 2030. EU Nanosafety Cluster. https://doi.org/10.5281/zenodo.1486012. doi:10.5281/zenodo.1486012.

View Article Online
DOI: 10.1039/D3EN00810J

11 Jeliazkova N, Apostolova MD, Andreoli C, Barone F, Barrick A, Battistelli C *et al.* Towards FAIR nanosafety data. *Nat Nanotechnol* 2021; **16**: 644–654.

12 Singh AV, Laux P, Luch A, Sudrik C, Wiehr S, Wild AM *et al.* Review of emerging concepts in nanotoxicology: opportunities and challenges for safer nanomaterial design. *Toxicol Mech Methods* 2019; **29**: 378–387.

13 Manke A, Wang L, Rojanasakul Y. Mechanisms of Nanoparticle-Induced Oxidative Stress and Toxicity. *Biomed Res Int* 2013; **2013**: 1–15.

14 Choi H, Choi B, Han J, Shin HE, Park W, Kim D. Reactive Oxygen Species Responsive Cleavable Hierarchical Metallic Supra-Nanostructure. *Small* 2022; **18**. doi:10.1002/smll.202202694.

15 Schwarz-Plaschg C, Kallhoff A, Eisenberger I. Making Nanomaterials Safer by Design? *Nanoethics* 2017; **11**: 277–281.

16 Jeliazkova N, Bleeker E, Cross R, Haase A, Janer G, Peijnenburg W *et al.* How can we justify grouping of nanoforms for hazard assessment? Concepts and tools to quantify similarity. *NanoImpact* 2022; **25**: 100366.

17 Kraegeloh A, Suarez-Merino B, Sluijters T, Micheletti C. Implementation of safe-by-design for nanomaterial development and safe innovation: Why we need a comprehensive approach. *Nanomaterials* 2018; **8**. doi:10.3390/nano8040239.

18 Bañares MA, Haase A, Tran L, Lobaskin V, Oberdörster G, Rallo R *et al.* CompNanoTox2015: novel perspectives from a European conference on computational nanotoxicology on predictive nanotoxicology. *Nanotoxicology* 2017; **11**: 839–845.

19 Stone V, Gottardo S, Bleeker EAJ, Braakhuis H, Dekkers S, Fernandes T *et al.* A framework for grouping and read-across of nanomaterials- supporting innovation and risk assessment. *Nano Today* 2020; **35**: 1–15.

20 Verdon R, Stone V, Murphy F, Christopher E, Johnston H, Doak S *et al.* The application of existing genotoxicity methodologies for grouping of nanomaterials: towards an integrated approach to testing and assessment. *Part Fibre Toxicol* 2022; **19**: 1–9.

21 Murphy FA, Johnston HJ, Dekkers S, Bleeker EAJ, Oomen AG, Fernandes TF *et al.* How to formulate hypotheses and IATAs to support grouping and read-across of nanoforms. *ALTEX* 2023; **40**: 125–140.

View Article Online
DOI: 10.1039/D3EN00810J

22 Sintes JR, Blázquez M, Moya S, socorro vazquez. Safety Issues and Regulatory Challenges of Nanomaterials A. 2012 doi:10.2788/76363.

23 Setyawati MI, Zhao Z, Ng KW. Transformation of Nanomaterials and Its Implications in Gut Nanotoxicology. *Small* 2020; **16**: 1–17.

24 Shirokii N, Din Y, Petrov I, Seregin Y, Sirotenko S, Razlivina J *et al.* Quantitative Prediction of Inorganic Nanomaterial Cellular Toxicity via Machine Learning. *Small* 2023; **19**: 1–7.

25 Godwin H, Nameth C, Avery D, Bergeson LL, Bernard D, Beryt E *et al.* Nanomaterial Categorization for Assessing Risk Potential To Facilitate Regulatory Decision-Making. *ACS Nano* 2015; **9**: 3409–3417.

26 Lynch I, Weiss C, Valsami-Jones E. A strategy for grouping of nanomaterials based on key physico-chemical descriptors as a basis for safer-by-design NMs. *Nano Today* 2014; **9**: 266–270.

27 Fischer I, Milton C, Wallace H. Toxicity testing is evolving! *Toxicol Res (Camb)* 2020; **9**: 67–80.

28 Schmeisser S, Miccoli A, von Bergen M, Berggren E, Braeuning A, Busch W *et al.* New approach methodologies in human regulatory toxicology – Not if, but how and when! *Environ Int* 2023; **178**: 108082.

29 Doak SH, Clift MJD, Costa A, Delmaar C, Gosens I, Halappanavar S *et al.* The Road to Achieving the European Commission's Chemicals Strategy for Nanomaterial Sustainability—A PATROLS Perspective on New Approach Methodologies. *Small* 2022; **18**. doi:10.1002/smll.202200231.

30 Bahl A, Ibrahim C, Plate K, Haase A, Dengjel J, Nymark P *et al.* PROTEOMAS: a workflow enabling harmonized proteomic meta-analysis and proteomic signature mapping. *J Cheminform* 2023; **15**: 1–17.

31 Padmore T, Stark C, Turkevich LA, Champion JA. Quantitative analysis of the role of fiber length on phagocytosis and inflammatory response by alveolar macrophages. *Biochimica et Biophysica Acta (BBA) - General Subjects* 2017; **1861**: 58–67.

32 Boyles MSP, Young L, Brown DM, MacCalman L, Cowie H, Moisala A *et al.* Multi-walled carbon nanotube induced frustrated phagocytosis, cytotoxicity and pro-inflammatory conditions in macrophages are length dependent and greater than that of asbestos. *Toxicology in Vitro* 2015; **29**: 1513–1528.

View Article Online
DOI: 10.1039/D3EN00810J

33 Nel A, Xia T, Meng H, Wang X, Lin S, Ji Z *et al.* Nanomaterial toxicity testing in the 21st century: Use of a predictive toxicological approach and high-throughput screening. *Acc Chem Res* 2013; **46**: 607–621.

34 Hsieh S, Bello D, Schmidt DF, Pal AK, Stella A, Isaacs JA *et al.* Mapping the Biological Oxidative Damage of Engineered Nanomaterials. *Small* 2013; **9**: 1853–1865.

35 Halappanavar S, Van Den Brule S, Nymark P, Gaté L, Seidel C, Valentino S *et al.* Adverse outcome pathways as a tool for the design of testing strategies to support the safety assessment of emerging advanced materials at the nanoscale. *Part Fibre Toxicol* 2020; **17**: 1–24.

36 Gerloff K, Landesmann B, Worth A, Munn S, Palosaari T, Whelan M. The Adverse Outcome Pathway approach in nanotoxicology. *Computational Toxicology* 2017; **1**: 3–11.

37 Labib S, Williams A, Yauk CL, Nikota JK, Wallin H, Vogel U *et al.* Nano-risk Science: Application of toxicogenomics in an adverse outcome pathway framework for risk assessment of multi-walled carbon nanotubes. *Part Fibre Toxicol* 2016; **13**: 1–17.

38 Cronin MTD, Bajot F, Enoch SJ, Madden JC, Roberts DW, Schwöbel J. The in chemico-in silico interface: Challenges for integrating experimental and computational chemistry to identify toxicity. *ATLA Alternatives to Laboratory Animals* 2009; **37**: 513–521.

39 Wachs IE. Number of surface sites and turnover frequencies for oxide catalysts. *J Catal* 2022; **405**: 462–472.

40 Lwin S, Li Y, Frenkel AI, Wachs IE. Nature of WOx Sites on SiO2 and Their Molecular Structure-Reactivity/Selectivity Relationships for Propylene Metathesis. *ACS Catal* 2016; **6**: 3061–3071.

41 J. M. Thomas, W. J. Thomas NY. *Principles and practice of heterogeneous catalysis*. VCH (1997). Page 27.

42 Briand LE, Hirt AM, Wachs IE. Quantitative determination of the number of surface active sites and the turnover frequencies for methanol oxidation over metal oxide catalysts: Application to bulk metal molybdates and pure metal oxide catalysts. *J Catal* 2001; **202**: 268–278.

43 Kulkarni D, Wachs IE. Isopropanol oxidation by pure metal oxide catalysts: Number of active surface sites and turnover frequencies. *Appl Catal A Gen* 2002; **237**: 121–137.

View Article Online
DOI: 10.1039/D3EN00810J

44 Briand LE, Jehng JM, Cornaglia L, Hirt AM, Wachs IE. Quantitative determination of the number of surface active sites and the turnover frequency for methanol oxidation over bulk metal vanadates. *Catal Today* 2003; **78**: 257–268.

45 Gates BC. *Catalytic chemistry*. 1991.

46 Tatibouët JM. Methanol oxidation as a catalytic surface probe. *Appl Catal A Gen* 1997; **148**: 213–252.

47 Jehng J-M, Wachs IE, Ford M. Temperature-Programmed (TP) Techniques. In: *Springer Handbook of Advanced Catalyst Characterization. Springer Handb. Chapter 45*. 2023, pp 1005–1029.

48 Wu Y, Gao F, Wang H, Kovarik L, Sudduth B, Wang Y. Probing Acid–Base Properties of Anatase TiO 2 Nanoparticles with Dominant {001} and {101} Facets Using Methanol Chemisorption and Surface Reactions. *The Journal of Physical Chemistry C* 2021; **125**: 3988–4000.

49 Jehng JM, Wachs IE, Patience GS, Dai YM. Experimental methods in chemical engineering: Temperature programmed surface reaction spectroscopy—TPSR. *Canadian Journal of Chemical Engineering* 2021; **99**: 423–434.

50 Daellenbach KR, Uzu G, Jiang J, Cassagnes LE, Leni Z, Vlachou A *et al.* Sources of particulate-matter air pollution and its oxidative potential in Europe. *Nature* 2020; **587**: 414–419.

51 Janssen NAH, Yang A, Strak M, Steenhof M, Hellack B, Gerlofs-Nijland ME *et al.* Oxidative potential of particulate matter collected at sites with different source characteristics. *Science of the Total Environment* 2014; **472**: 572–581.

52 Gao D, Ripley S, Weichenthal S, Godri Pollitt KJ. Ambient particulate matter oxidative potential: Chemical determinants, associated health effects, and strategies for risk management. *Free Radic Biol Med* 2020; **151**: 7–25.

53 Breznan D, Nazemof N, Kunc F, Hill M, Vladisavljevic D, Gomes J *et al.* Acellular oxidative potential assay for screening of amorphous silica nanoparticles. *Analyst* 2020; **145**: 4867–4879.

54 Rao L, Zhang L, Wang X, Xie T, Zhou S, Lu S *et al.* Oxidative potential induced by ambient particulate matters with acellular assays: A review. *Processes* 2020; **8**: 1–21.

View Article Online
DOI: 10.1039/D3EN00810J

55 Kramer AL, Dorn S, Perez A, Roper C, Titaley IA, Cayton K *et al.* Assessing the oxidative potential of PAHs in ambient PM2.5 using the DTT consumption assay. *Environmental Pollution* 2021; **285**: 117411.

56 Jeevanandam J, Barhoum A, Chan YS, Dufresne A, Danquah MK. Review on nanoparticles and nanostructured materials: History, sources, toxicity and regulations. *Beilstein Journal of Nanotechnology* 2018; **9**: 1050–1074.

57 Yang H, Liu C, Yang D, Zhang H, Xi Z. Comparative study of cytotoxicity, oxidative stress and genotoxicity induced by four typical nanomaterials: The role of particle size, shape and composition. *Journal of Applied Toxicology* 2009; **29**: 69–78.

58 Setyawati MI, Tay CY, Leong DT. Effect of zinc oxide nanomaterials-induced oxidative stress on the p53 pathway. *Biomaterials* 2013; **34**: 10133–10142.

59 Čapek J, Roušar T. Detection of oxidative stress induced by nanomaterials in cells—the roles of reactive oxygen species and glutathione. *Molecules* 2021; **26**. doi:10.3390/molecules26164710.

60 Mendoza RP, Brown JM. Engineered nanomaterials and oxidative stress: Current understanding and future challenges. *Curr Opin Toxicol* 2019; **13**: 74–80.

61 Crobeddu B, Aragao-Santiago L, Bui LC, Boland S, Baeza Squiban A. Oxidative potential of particulate matter 2.5 as predictive indicator of cellular stress. *Environmental Pollution* 2017; **230**: 125–133.

62 Jiang H, Sabbir Ahmed CM, Canchola A, Chen JY, Lin YH. Use of dithiothreitol assay to evaluate the oxidative potential of atmospheric aerosols. *Atmosphere (Basel)* 2019; **10**: 1–21.

63 Øvrevik J. Oxidative Potential Versus Biological Effects: A Review on the Relevance of Cell-Free/Abiotic Assays as Predictors of Toxicity from Airborne Particulate Matter. *Int J Mol Sci* 2019; **20**: 4772.

64 Crobeddu B, Baudrimont I, Deweirdt J, Sciare J, Badel A, Camproux AC *et al.* Lung Antioxidant Depletion: A Predictive Indicator of Cellular Stress Induced by Ambient Fine Particles. *Environ Sci Technol* 2020; **54**: 2360–2369.

65 Sauvain JJ, Deslarzes S, Riediker M. Nanoparticle reactivity toward dithiothreitol. *Nanotoxicology* 2008; **2**: 121–129.

66 Sauvain JJ, Rossi MJ, Riediker M. Comparison of three acellular tests for assessing the oxidation potential of nanomaterials. *Aerosol Science and Technology* 2013; **47**: 218–227.

View Article Online
DOI: 10.1039/D3EN00810J

67 Briand LE, Hirt AM, Wachs IE. Quantitative determination of the number of surface active sites and the turnover frequencies for methanol oxidation over metal oxide catalysts: Application to bulk metal molybdates and pure metal oxide catalysts. *J Catal* 2001; **202**: 268–278.

68 Wachs IE. Number of surface sites and turnover frequencies for oxide catalysts. *J Catal* 2022; **405**: 462–472.

69 Jensen KA. NanoGenoTox. WP4, Deliverable 3: Final protocol for producing suitable MN exposure media. The generic NANOGENOTOX dispersion protocol. Standard Operation Procedure (SOP) and background documentation. 2011.

70 JRC NANOMATERIALS REPOSITORY. List of Representative Nanomaterials. 2016.

71 Rasmussen K, Mast J, Temmerman P De, Verleysen E, Waegeneers N, Steen F Van *et al. Titanium Dioxide, NM-100, NM-101, NM-102, NM-103, NM-104, NM-105: Characterisation and Physico- Chemical Properties*. 2014 doi:10.2788/79554.

72 Singh C, Europäische Kommission Gemeinsame Forschungsstelle Institute for Health and Consumer Protection. *Cerium Dioxide NM-211, NM-212, NM-213, characterisation and test item preparation JRC repository: NM-series of representative manufactured nanomaterials*. 2014 doi:10.2788/80203.

73 Singh C, Friedrichs S, Levin M, Birkedal R, Jensen KA, Pojana G *et al. Zinc Oxide NM-110, NM-111, NM-112, NM-113 Characterisation and Test Item Preparation*. 2011 doi:10.2787/55008.

74 Martín-Gómez J, Hidalgo-Carrillo J, Montes V, Estévez-Toledano RC, Escamilla JC, Marinas A *et al.* EPR and CV studies cast further light on the origin of the enhanced hydrogen production through glycerol photoreforming on CuO:TiO2 physical mixtures. *J Environ Chem Eng* 2021; **9**: 105336.

75 Kochev N, Jeliazkova N, Paskaleva V, Tancheva G, Iliev L, Ritchie P *et al.* Your spreadsheets can be fair: A tool and fairification workflow for the enanomapper database. *Nanomaterials* 2020; **10**: 1–23.

76 Hastings J, Jeliazkova N, Owen G, Tsiliki G, Munteanu CR, Steinbeck C *et al.* eNanoMapper: Harnessing ontologies to enable data integration for nanomaterial risk assessment. *J Biomed Semantics* 2015; **6**: 1–15.

77 Moschini E, Colombo G, Chirico G, Capitani G, Dalle-Donne I, Mantecca P. Biological mechanism of cell oxidative stress and death during short-term exposure to nano CuO. *Sci Rep* 2023; **13**: 2326.

View Article Online
DOI: 10.1039/D3EN00810J

78 Moschini E, Gualtieri M, Colombo M, Fascio U, Camatini M, Mantecca P. The modality of cell-particle interactions drives the toxicity of nanosized CuO and TiO2 in human alveolar epithelial cells. *Toxicol Lett* 2013; **222**: 102–116.

79 Semisch A, Ohle J, Witt B, Hartwig A. Cytotoxicity and genotoxicity of nano - and microparticulate copper oxide: role of solubility and intracellular bioavailability. *Part Fibre Toxicol* 2014; **11**: 10.

80 Kwon J-T, Kim Y, Choi S, Yoon B, Kim H-S, Shim I *et al.* Pulmonary Toxicity and Proteomic Analysis in Bronchoalveolar Lavage Fluids and Lungs of Rats Exposed to Copper Oxide Nanoparticles. *Int J Mol Sci* 2022; **23**: 13265.

81 Perelshtein I, Lipovsky A, Perkas N, Gedanken A, Moschini E, Mantecca P. The influence of the crystalline nature of nano-metal oxides on their antibacterial and toxicity properties. *Nano Res* 2015; **8**: 695–707.

82 Mouche I, Malésic L, Gillardeaux O. FETAX assay for evaluation of developmental toxicity. *Methods in Molecular Biology* 2017; **1641**: 311–324.

83 Ahmad J, Alhadlaq HA, Alshamsan A, Siddiqui MA, Saquib Q, Khan ST *et al.* Differential cytotoxicity of copper ferrite nanoparticles in different human cells. *Journal of Applied Toxicology* 2016; **36**: 1284–1293.

84 Precupas A, Gheorghe D, Botea-Petcu A, Leonties AR, Sandu R, Popa VT *et al.* Thermodynamic Parameters at Bio-Nano Interface and Nanomaterial Toxicity: A Case Study on BSA Interaction with ZnO, SiO2, and TiO2. *Chem Res Toxicol* 2020; **33**: 2054–2071.

85 Yamani N El, Collins AR, Rundén-Pran E, Fjellsbø LM, Shaposhnikov S, Zienolddiny S *et al.* In vitro genotoxicity testing of four reference metal nanomaterials, titanium dioxide, zinc oxide, cerium oxide and silver: Towards reliable hazard assessment. *Mutagenesis* 2017; **32**: 117–126.

86 Farcal L, Andón FT, Di Cristo L, Rotoli BM, Bussolati O, Bergamaschi E *et al.* Comprehensive in vitro toxicity testing of a panel of representative oxide nanomaterials: First steps towards an intelligent testing strategy. *PLoS One* 2015; **10**: 1–34.

87 Kermanizadeh A, Pojana G, Gaiser BK, Birkedal R, Bilaničová D, Wallin H *et al.* In vitro assessment of engineered nanomaterials using a hepatocyte cell line: Cytotoxicity, pro-inflammatory cytokines and functional markers. *Nanotoxicology* 2013; **7**: 301–313.

View Article Online
DOI: 10.1039/D3EN00810J

88 Driessen MD, Mues S, Vennemann A, Hellack B, Bannuscher A, Vimalakanthan V *et al.* Proteomic analysis of protein carbonylation: A useful tool to unravel nanoparticle toxicity mechanisms. *Part Fibre Toxicol* 2015; **12**: 1–18.

89 Cao Y, Roursgaard M, Kermanizadeh A, Loft S, Møller P. Synergistic effects of zinc oxide nanoparticles and fatty acids on toxicity to caco-2 cells. *Int J Toxicol* 2015; **34**: 67–76.

90 Gu Y, Cheng S, Chen G, Shen Y, Li X, Jiang Q *et al.* The effects of endoplasmic reticulum stress inducer thapsigargin on the toxicity of ZnO or TiO2 nanoparticles to human endothelial cells. *Toxicol Mech Methods* 2017; **27**: 191–200.

91 Thongkam W, Gerloff K, van Berlo D, Albrecht C, Schins RPF. Oxidant generation, DNA damage and cytotoxicity by a panel of engineered nanomaterials in three different human epithelial cell lines. *Mutagenesis* 2017; **32**: 105–115.

92 Zijno A, Cavallo D, Di Felice G, Ponti J, Barletta B, Butteroni C *et al.* Use of a common European approach for nanomaterials' testing to support regulation: a case study on titanium and silicon dioxide representative nanomaterials. *Journal of Applied Toxicology* 2020; **40**: 1511–1525.

93 Nel AE, Mädler L, Velegol D, Xia T, Hoek EMV, Somasundaran P *et al.* Understanding biophysicochemical interactions at the nano-bio interface. *Nat Mater* 2009; **8**: 543–557.

94 Xia T, Kovochich M, Liong M, Mädler L, Gilbert B, Shi H *et al.* Comparison of the mechanism of toxicity of zinc oxide and cerium oxide nanoparticles based on dissolution and oxidative stress properties. *ACS Nano* 2008; **2**: 2121–2134.

95 Sauer UG, Vogel S, Aumann A, Hess A, Kolle SN, Ma-Hock L *et al.* Applicability of rat precision-cut lung slices in evaluating nanomaterial cytotoxicity, apoptosis, oxidative stress, and inflammation. *Toxicol Appl Pharmacol* 2014; **276**: 1–20.

96 Srinivas A, Rao PJ, Selvam G, Murthy PB, Reddy PN. Acute inhalation toxicity of cerium oxide nanoparticles in rats. *Toxicol Lett* 2011; **205**: 105–115.

97 Demokritou P, Gass S, Pyrgiotakis G, Cohen JM, Goldsmith W, McKinney W *et al.* An in vivo and in vitro toxicological characterisation of realistic nanoscale CeO2 inhalation exposures. *Nanotoxicology* 2013; **7**: 1338–1350.

98 Wiemann M, Vennemann A, Sauer UG, Wiench K, Ma-Hock L, Landsiedel R. An in vitro alveolar macrophage assay for predicting the short-term inhalation toxicity of nanomaterials. *J Nanobiotechnology* 2016; **14**: 16.

View Article Online
DOI: 10.1039/D3EN00810J

99 Solorio-Rodríguez A, Escamilla-Rivera V, Uribe-Ramírez M, González-Pozos S, Hernández-Soto J, Rafael-Vázquez L *et al.* In vitro cytotoxicity study of superparamagnetic iron oxide and silica nanoparticles on pneumocyte organelles. *Toxicology in Vitro* 2021; **72**: 105071.

100 Cavallo D, Ciervo A, Fresegna AM, Maiello R, Tassone P, Buresti G *et al.* Investigation on cobalt-oxide nanoparticles cyto-genotoxicity and inflammatory response in two types of respiratory cells. *Journal of Applied Toxicology* 2015; **35**: 1102–1113.

101 Lugun O, Singh J, Singh Thakur R, Pandey AK. Cobalt oxide (Co 3 O 4) nanoparticles induced genotoxicity in Chinese hamster lung fibroblast (V79) cells through modulation of reactive oxygen species. *Mutagenesis* 2022; **37**: 44–59.

102 Marucco A, Carella E, Fenoglio I. A comparative study on the efficacy of different probes to predict the photo-activity of nano-titanium dioxide toward biomolecules. *RSC Adv* 2015; **5**: 89559–89568.

103 Davydov A. *Molecular Spectroscopy of Oxide Catalyst Surfaces*. Wiley, 2003 doi:10.1002/0470867981.

104 Collins SE, Briand LE, Gambaro LA, Baltanás MA, Bonivardi AL. Adsorption and Decomposition of Methanol on Gallium Oxide Polymorphs. *The Journal of Physical Chemistry C* 2008; **112**: 14988–15000.

105 Bazin P, Thomas S, Marie O, Daturi M. New insights into the methanol oxidation mechanism over Au/CeO2 catalyst through complementary kinetic and FTIR operando SSITKA approaches. *Catal Today* 2012; **182**: 3–11.

106 Bahl A, Hellack B, Wiemann M, Giusti A, Werle K, Haase A *et al.* Nanomaterial categorization by surface reactivity: A case study comparing 35 materials with four different test methods. *NanoImpact* 2020; **19**: 100234.

107 Hellack B, Nickel C, Schins RPF. Oxidative potential of silver nanoparticles measured by electron paramagnetic resonance spectroscopy. *Journal of Nanoparticle Research* 2017; **19**: 404.

108 Wu Z, Li M, Howe J, Meyer HM, Overbury SH. Probing defect sites on CeO2 nanocrystals with well-defined surface planes by raman spectroscopy and O2 adsorption. *Langmuir* 2010; **26**: 16595–16606.

109 Pushkarev V V., Kovalchuk VI, D'Itri JL. Probing defect sites on the CeO2 surface with dioxygen. *Journal of Physical Chemistry B* 2004; **108**: 5341–5348.

View Article Online
DOI: 10.1039/D3EN00810J

110 Wang Q, Li Y, Serrano-Lotina A, Han W, Portela R, Wang R *et al.* Operando Investigation of Toluene Oxidation over 1D Pt@CeO 2 Derived from Pt Cluster-Containing MOF. *J Am Chem Soc* 2021; **143**: 196–205.

111 Wyrwoll AJ, Lautenschläger P, Bach A, Hellack B, Dybowska A, Kuhlbusch TAJ *et al.* Size matters - The phototoxicity of TiO2 nanomaterials. *Environmental Pollution* 2016; **208**: 859–867.

112 Marucco A, Carella E, Fenoglio I. A comparative study on the efficacy of different probes to predict the photo-activity of nano-titanium dioxide toward biomolecules. *RSC Adv* 2015; **5**: 89559–89568.

113 Zhang H, Ji Z, Xia T, Meng H, Low-Kam C, Liu R *et al.* Use of Metal Oxide Nanoparticle Band Gap To Develop a Predictive Paradigm for Oxidative Stress and Acute Pulmonary Inflammation. *ACS Nano* 2012; **6**: 4349–4368.

114 Arakha M, Roy J, Nayak PS, Mallick B, Jha S. Zinc oxide nanoparticle energy band gap reduction triggers the oxidative stress resulting into autophagy-mediated apoptotic cell death. *Free Radic Biol Med* 2017; **110**: 42–53.

115 Paruthi A, Brown JM, Panda E, Gautam ARS, Singh S, Misra SK. Transformation in band energetics of CuO nanoparticles as a function of solubility and its impact on cellular response. *NanoImpact* 2021; **22**. doi:10.1016/j.impact.2021.100324.

116 Çetin YA, Martorell B, Serratosa F, Aguilera-Porta N, Calatayud M. Analyzing the TiO 2 surface reactivity based on oxygen vacancies computed by DFT and DFTB methods. *Journal of Physics: Condensed Matter* 2022; **34**: 314004.

117 Chou H-H, Ya-Hsuan Liou S, Calatayud M. Modelling rutile TiO2nanorod growth preferences: A density functional theory study. *Catal Today* 2020; **356**: 49–55.

118 Mancardi G, Mikolajczyk A, Annapoorani VK, Bahl A, Blekos K, Burk J *et al.* A computational view on nanomaterial intrinsic and extrinsic features for nanosafety and sustainability. *Materials Today* 2023; **67**: 344–370.

119 Dumit VI, Ammar A, Bakker MI, Bañares MA, Bossa C, Costa A *et al.* From principles to reality. FAIR implementation in the nanosafety community. *Nano Today* 2023; **51**: 101923.

120 Moschini E, Gualtieri M, Colombo M, Fascio U, Camatini M, Mantecca P. The modality of cell-particle interactions drives the toxicity of nanosized CuO and TiO2 in human alveolar epithelial cells. *Toxicol Lett* 2013; **222**: 102–116.

View Article Online
DOI: 10.1039/D3EN00810J

121 Simeone FC, Costa AL. Assessment of cytotoxicity of metal oxide nanoparticles on the basis of fundamental physical-chemical parameters: A robust approach to grouping. *Environ Sci Nano* 2019; **6**: 3102–3112.

122 Reinosa JJ, Rojo MM, del Campo A, Martín-González M, Fernández JF. Highly Efficient Antimicrobial Ceramics Based on Electrically Charged Interfaces. *ACS Appl Mater Interfaces* 2019; **11**: 39254–39262.

123 Zuo L, Wijegunawardana D. Redox Role of ROS and Inflammation in Pulmonary Diseases. In: *Advances in Experimental Medicine and Biology*. 2021, pp 187–204.

124 Cuillel M, Chevallet M, Charbonnier P, Fauquant C, Pignot-Paintrand I, Arnaud J *et al.* Interference of CuO nanoparticles with metal homeostasis in hepatocytes under sub-toxic conditions. *Nanoscale* 2014; **6**: 1707–1715.

125 Mantecca P, Moschini E, Chirico G, Capitani G. Surface bio-interactions stand at the base of the short-term nano CuO-induced cell oxidative stress: insights for a safe(r)-by-design approach. 2022. doi:10.21203/rs.3.rs-1306935/v2.

126 Semisch A, Ohle J, Witt B, Hartwig A. Cytotoxicity and genotoxicity of nano - and microparticulate copper oxide: Role of solubility and intracellular bioavailability. *Part Fibre Toxicol* 2014; **11**. doi:10.1186/1743-8977-11-10.

127 Strauch BM, Niemand RK, Winkelbeiner NL, Hartwig A. Comparison between micro- and nanosized copper oxide and water soluble copper chloride: Interrelationship between intracellular copper concentrations, oxidative stress and DNA damage response in human lung cells. *Part Fibre Toxicol* 2017; **14**. doi:10.1186/s12989-017-0209-1.

128 Diabaté S, Armand L, Murugadoss S, Dilger M, Fritsch-Decker S, Schlager C *et al.* Air–liquid interface exposure of lung epithelial cells to low doses of nanoparticles to assess pulmonary adverse effects. *Nanomaterials* 2021; **11**: 1–23.

129 Wu Z, Li M, Mullins DR, Overbury SH. Probing the surface sites of CeO 2 nanocrystals with well-defined surface planes via methanol adsorption and desorption. *ACS Catal* 2012; **2**: 2224–2234.

130 Wu Z, Li M, Howe J, Meyer HM, Overbury SH. Probing defect sites on CeO2 nanocrystals with well-defined surface planes by raman spectroscopy and O2 adsorption. *Langmuir* 2010; **26**: 16595–16606.

131 Trovarelli A. Catalysis by Ceria and Related Materials. 2002; **2**. doi:10.1142/P249.

View Article Online
DOI: 10.1039/D3EN00810J

132 Tran L, Bañares MA, Rallo R. *Modelling the Toxicity of Nanoparticles*. Springer International Publishing: Cham, 2017 doi:10.1007/978-3-319-47754-1.

133 Ziemba M, Schilling C, Ganduglia-Pirovano MV, Hess C. Toward an Atomic-Level Understanding of Ceria-Based Catalysts: When Experiment and Theory Go Hand in Hand. *Acc Chem Res* 2021; **54**: 2884–2893.

134 Schilling C, Hofmann A, Hess C, Ganduglia-Pirovano MV. Raman Spectra of Polycrystalline CeO2: A Density Functional Theory Study. *Journal of Physical Chemistry C* 2017; **121**: 20834–20849.

135 Ziemba M, Ganduglia-Pirovano MV, Hess C. Elucidating the Oxygen Storage-Release Dynamics in Ceria Nanorods by Combined Multi-Wavelength Raman Spectroscopy and DFT. *Journal of Physical Chemistry Letters* 2020; **11**: 8554–8559.

136 Mittal S, Pandey AK. Cerium Oxide Nanoparticles Induced Toxicity in Human Lung Cells: Role of ROS Mediated DNA Damage and Apoptosis. *Biomed Res Int* 2014; **2014**: 1–14.

137 Keller J, Wohlleben W, Ma-Hock L, Strauss V, Gröters S, Küttler K *et al.* Time course of lung retention and toxicity of inhaled particles: short-term exposure to nano-Ceria. *Arch Toxicol* 2014; **88**: 2033–2059.

138 Jiang P, Zhang L, Liu X, Ye C, Zhu P, Tan T *et al.* Tuning oxidant and antioxidant activities of ceria by anchoring copper single-site for antibacterial application. *Nature Communications 2024 15:1* 2024; **15**: 1–15.

139 Fragou F, Zindrou A, Deligiannakis Y, Louloudi M. Engineering of Oxygen-Deficient Nano-CeO 2−x with Tunable Biocidal and Antioxidant Activity. *Cite This: ACS Appl Nano Mater* 2024; **7**: 10552–10564.

140 Wang Q, Yeung KL, Bañares MA. Operando Raman-online FTIR investigation of ceria, vanadia/ceria and gold/ceria catalysts for toluene elimination. *J Catal* 2018; **364**: 80–88.

141 Wang Q, Li Y, Serrano-Lotina A, Han W, Portela R, Wang R *et al.* Operando Investigation of Toluene Oxidation over 1D Pt@CeO2Derived from Pt Cluster-Containing MOF. *J Am Chem Soc* 2021; **143**: 196–205.

142 Heckert EG, Seal S, Self WT. Fenton-like reaction catalyzed by the rare earth inner transition metal cerium. *Environ Sci Technol* 2008; **42**: 5014–5019.

View Article Online
DOI: 10.1039/D3EN00810J

143 Xue Y, Luan Q, Yang D, Yao X, Zhou K. Direct evidence for hydroxyl radical scavenging activity of cerium oxide nanoparticles. *Journal of Physical Chemistry C* 2011; **115**: 4433–4438.

144 Hardas SS, Dan M, Florence RL, Wu P, Grulke EA, Tseng MT *et al.* Rat brain pro-oxidant effects of peripherally administered 5 nm ceria 30 days after exposure. 2012. doi:10.1016/j.neuro.2012.06.007.

145 Zhang P, Ma Y, Zhang Z, He X, Zhang J, Guo Z *et al.* Biotransformation of ceria nanoparticles in cucumber plants. *ACS Nano* 2012; **6**: 9943–9950.

146 Shi X, Liu Q, Gong Z, Jin Z, Guo H, Wen X *et al.* Vacancy-rich Fe-Ce mixed oxides as nanoenzymes for efficient antioxidant activity in vitro. *Appl Surf Sci* 2024; **664**: 160256.

147 Driessen MD, Mues S, Vennemann A, Hellack B, Bannuscher A, Vimalakanthan V *et al.* Proteomic analysis of protein carbonylation: A useful tool to unravel nanoparticle toxicity mechanisms. *Part Fibre Toxicol* 2015; **12**: 1–18.

148 Cohen J, Ji Z, Xia T, Demokritou P. An integrated approach for the in vitro dosimetry of engineered nanomaterials : Relevant in vitro dose (RID) functions Background (1 of 2). *Part Fibre Toxicol* 2014; **11**: 1–12.

149 Hull M, Kennedy AJ, Detzel C, Vikesland P, Chappell MA. Moving beyond mass: The unmet need to consider dose metrics in environmental nanotoxicology studies. *Environ Sci Technol* 2012; **46**: 10881–10882.

150 Fenoglio I, Tomatis M, Lison D, Muller J, Fonseca A, Nagy JB *et al.* Reactivity of carbon nanotubes: Free radical generation or scavenging activity? *Free Radic Biol Med* 2006; **40**: 1227–1233.